Determination of Structural and Optical Properties of Zn₁₋ₓCuₓO Nanoparticles by Chemical Bath Deposition Waste Recovery Technique

Emin Yakar[1,*]

[1] Department of Materials Science and Engineering, Faculty of Engineering, Çanakkale Onsekiz Mart University, Çanakkale, Türkiye

Abstract − The present study was conducted to obtain Cu:ZnO nanoparticles by precipitation technique from chemical bath deposition wastes and to characterize the samples by various techniques to determine their size, morphology, band gap and defect energy states. In this work, $Zn_{1-x}Cu_xO$ nanoparticles (x= 0.025, x=0.050, and x=0.075) were synthesized by co-precipitation technique using chemical bath deposition wastes of Cu:ZnO thin films. The XRD evaluation showed that the well-crystalline hexagonal wurtzite ZnO indexed peaks. Average crystallite sizes were found to be around 35.6-42.9 nm range by using the Debye-Scherrer equation. Surface morphology results showed that dense layer of nano-roses and less nanorods formations in low Cu-concentrated (x=0.025 and x=0.050) samples. The optical absorption edge shifted slightly to the higher wavelength from 350 nm to 375 nm with decreasing copper concentration, as mentioned the blue shift. Blue shift might be caused an increase in optical band gap from 3.14 eV to 3.28 eV due to the decrease in Cu concentration. In this study, the preferred co-precipitation technique was performed by using the wastes of chemical bath deposition. This work aims to produce high quality Cu:ZnO nanoparticles and investigate their optical properties by using "Chemical Bath Deposition" wastes of Cu:ZnO films. In this way, the recovery of chemical bath deposition waste and the production of thin films and nanoparticles from a single solution might be possible.

Keywords − Nanoparticle synthesis, optical band gap, oxygen vacancy, waste recovery

1. Introduction

Although hazardous waste represents a very small proportion of all waste produced in Europe, they possess different risks on the human health and environment. Especially, recovery of solvent and chemical wastes (liquid, semi-solid and solid forming) is a serious problem in chemical laboratories. Recycling can be done by returning chemicals stored in labeled containers to the original supplier, or by donating them to academic institutions that may have a legitimate need, or by converting them into products that have a legitimate use. Chemical bath deposition (CBD) is the most preferred technique in chemical thin film production due to its simplicity, inexpensive and lack of installation. However, storage of the remaining toxic waste solutions which occurred during the production process result storage and health problems. Furthermore, excess waste solvents and precipitation production can be seen as the major problems for CBD technique in industrial scale applications (Chu et al., 2021). In order to solve this significant problem, Wang has a patent that proposed waste liquid recovery system for CBD (Wang, 2019). In CdS thin layer synthesis, more than 90% of ammonia has been recovered and purified enough to be recycled directly to formulate new baths. In addition, recycling of cadmium was achieved by leaching of solid cadmium compounds and cadmium electrowinning, as investigated by (Malinowska et.al., 2002). In this work, the residues of chemical bath waste that collapses

[1] ⓘ eyakar@comu.edu.tr
*Corresponding Author

to the bottom has been used in nanoparticle synthesis, as in the same co-precipitation technique. The optical properties of Cu:ZnO nanoparticles have been studied by many researchers. Cu-doped ZnO nanoparticles has a broad peak at 505 nm in PL spectrum so the enhanced visible light optical activity can be observed (Vasudevan et al., 2020). Naik et.al. investigated that Cu:ZnO nanoparticles have violet (423 nm) and blue (478 nm) emissions with changing optical band gap altering Cu concentration although Cu-concentration has no obvious effect on the PL spectrum (Naik et al., 2021). Tuning of crystallite size and shape, the distortion of the host lattice, blue shift of absorption edge and energy gap (3.66 eV to 3.99 eV) was reported by Cu addition, as explained by (Anita et.al., 2020). It is known that, blue shift is so beneficial for opto-electronic device and light-emitting diode applications (Debanath et al., 2013).

2. Materials and Methods

In this study simple co-precipitation was performed by using the wastes of chemical bath deposition applied solutions. All chemicals had high purity (> 99%) and purchased from Sigma-Aldrich. Detailed Cu:ZnO thin film synthesis by using chemical bath was explained in our previous study (Sarf et al., 2021). The waste solutions obtained from this study were kept for one day.As shown in Figure 1, precipitation was centrifuged and then washed by ethanol and distilled water for several times to remove surface impurities. All products were annealed at 500 °C for two hours. In the $Zn_{1-x}Cu_xO$ nanoparticle samples, x is 0.025, 0.050 and 0.0075. Structural characterization was determined by Rigaku SmartLab X-ray diffractometer employing CuKα (1.5406 Å) radiation which operated under 40 mA and 45 kV with using powder method. Surface morphology of the samples was investigated by JEOL JSM- 7100F-SEM (Scanning Electron Microscope). Elemental microanalysis (wt%) of nanocomposites was determined by OXFORD Instruments X-Max EDX (energy-dispersive X-ray spectrometer) which had been attached to SEM. The optical properties were recorded in 300-900 nm range and examined by using Analytical Jena Uv-Vis spectroscopy.
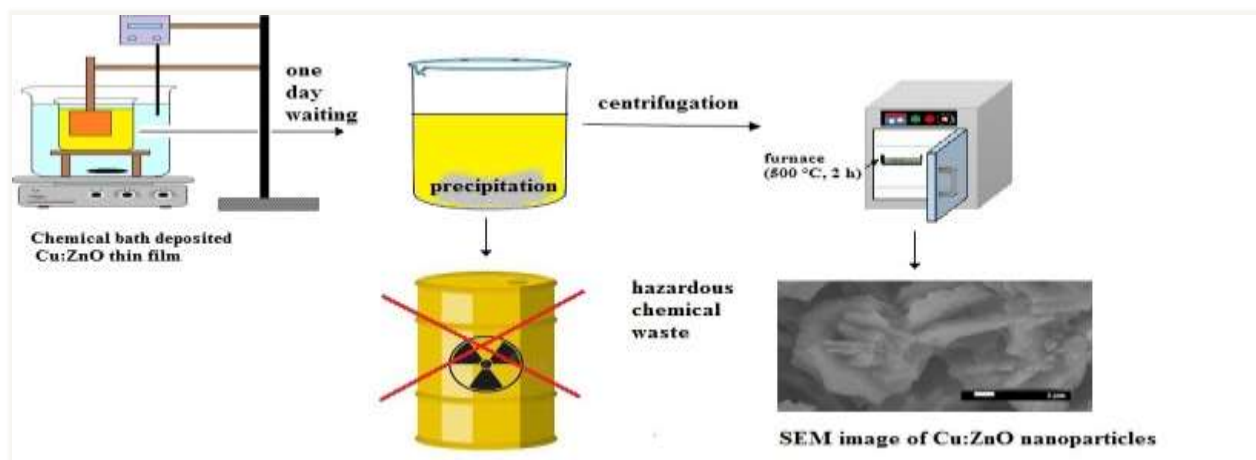

Figure 1. Experimental setup demonstration

3. Results and Discussion

3.1. Structural Properties

Structural characterization and structural parameters were determined by using x-ray patterns in the 2θ=20°-80° range. All of the samples had hexagonal würtzite ZnO structure, as shown in Fig. 2 and typical ZnO indexed peaks of (001), (002) and (101) were observed, according to JCPDS Card No: 36-1451 without impurity. A slightly shift was not detected by increasing Cu concentration from 2θ values due to Cu^{2+} (0.73 Å) ions were substituted with Zn^{2+}(0.74 Å) ions due to the ionic radius Cu^{2+} is so close to Zn^{2+} compared to pure ZnO sample from previous study (Vasudevan et. al., 2021). In the literature, the copper in ZnO is diavalent (Das et al., 2017). Cu incorporation into ZnO lattice caused a decrease in ZnO crystallinity compared to reference pure ZnO. In addition an increase in the lattice disorder and imperfections caused by Cu^{2+} ions replacement with Zn^{2+} ions, as shown in similar study by (Vasudevan et.al., 2021). By the

increasing Cu ratio from x=0.025 to x=0.075 resulted in thermodynamically favorable (002) intensity increased with improving crystallinity. Preferential orientation of the samples had (101) peak.
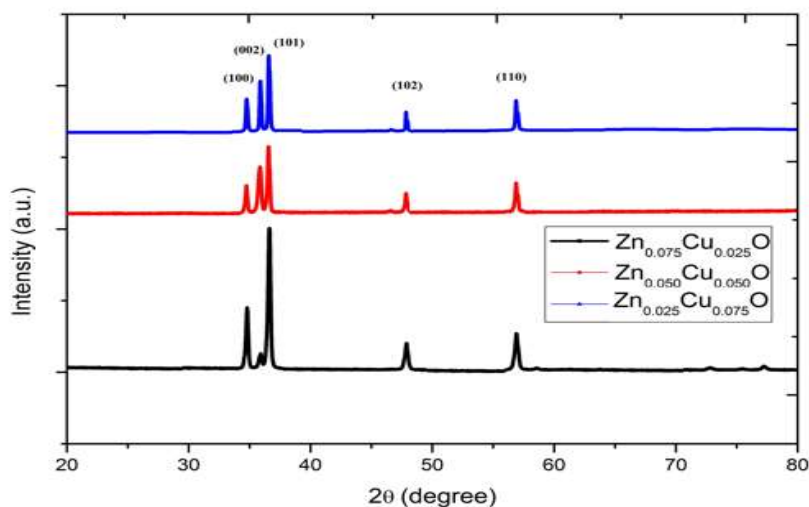

Figure 2. X-ray patterns of $Zn_{0.025}Cu_{0.075}O$, $Zn_{0.050}Cu_{0.050}O$ and $Zn_{0.075}Cu_{0.025}O$ nanoparticles

Structural parameters of the samples have been shown in Table 1. The average particle size of the samples (D) was measured by Debye-Scherrer equation without strain effect, as shown in Equation (3.1);

$$D = \frac{0.94\,\lambda}{\beta_{hkl}cos\theta} \tag{3.1}$$

Microstrain (ε) of the samples was calculated by Equation (3.2);

$$\beta_{hkl}cos\theta = 4\varepsilon sin\theta \tag{3.2}$$

In addition, dislocation density (δ) which is a measure of the amount of defects in the crystal was measured by Equation (3.3);

$$\delta = 1/D^2 \tag{3.3}$$

where λ is the wavelength of x-ray radiation, β is the full width at half maximum (FWHM) and θ is diffraction angle and ε is the strain.

No major change was observed in the strong peaks with the addition of copper. This may be due to the displacement of copper atoms by zinc in the hexagonal lattice, the separation of copper into the non-crystalline region at the grain boundaries.

Table 1
Structural parameters of $Zn_{0.025}Cu_{0.075}O$, $Zn_{0.050}Cu_{0.050}O$ and $Zn_{0.075}Cu_{0.025}O$ nanoparticles

	2θ (°)	d (Å)	D (nm)	Microstrain (ε) (%)	Δ (nm⁻²) (10⁻⁴)
$Zn_{0.075}Cu_{0.025}O$	36.63	2.4511	35.6	5.479	7.89
$Zn_{0.050}Cu_{0.050}O$	36.57	2.4568	40.2	5.160	6.22
$Zn_{0.025}Cu_{0.075}O$	36.53	2.4575	42.9	4.993	5.43

Measured structural parameters according to preferential orientation (101) peak were shown in Table 1.

Average crystallite size increased with the increasing of Cu concentration in the host ZnO, and it could be attributed to heterogeneous crystal growth at low supersaturation and crystals could grow faster than they nucleate, which result in a larger crystal size distribution (Istrate et al., 2021). c/a value of 1.48 was smaller than ideal c/a value of 1.63 due to the substitution of Cu into ZnO which indicated the electronegativity difference between Zn and Cu (Labhane et al., 2015).
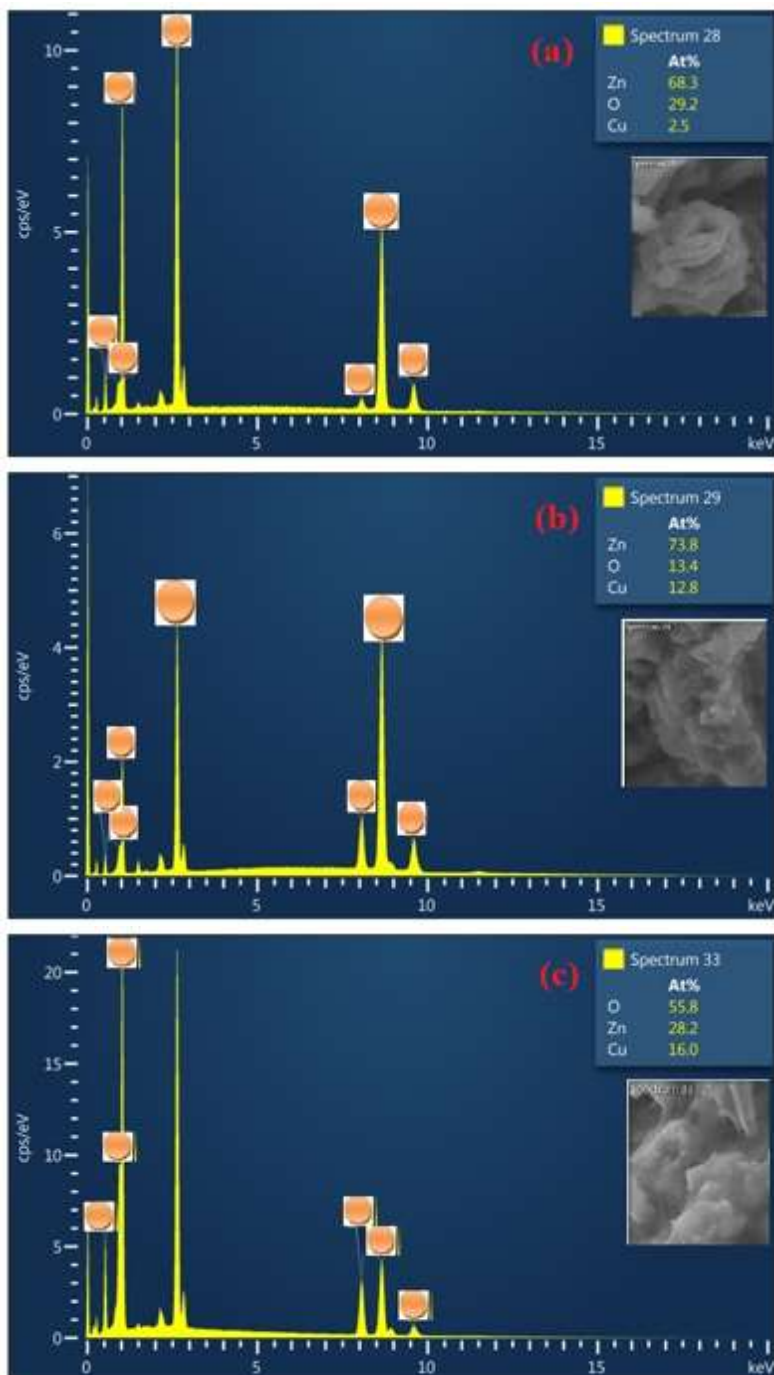
3.2. Elemental Analysis

Figure 3. Elemental analysis results of (a) $Zn_{0.075}Cu_{0.025}O$, (b)$Zn_{0.050}Cu_{0.050}O$ and (c) $Zn_{0.025}Cu_{0.075}O$ nanoparticles.

The presence of elements Zn, O and Cu (%w) was shown in Fig.3 . No impurity signal was detected from solution based with Zn, Cu and O elements signals were detected. . The characteristic peaks of O appeared at

0.5 keV while the characteristic peaks of Zn appeared at 1 and 8.7 keV. The Cu signal at 8.04 keV was observed in the synthesized samples. Similar results were obtained in our previous study (Sarf et.al., 2021).

3.3. Surface Morphologies

Surface morphology of the samples were shown in Fig.4. No crack formation was detected and nano-rose type forms and nanorods were shown in $Zn_{0.025}Cu_{0.075}O$ and $Zn_{0.050}Cu_{0.050}O$ nanoparticles which implied growth process was similar for both of the precipitated particles.
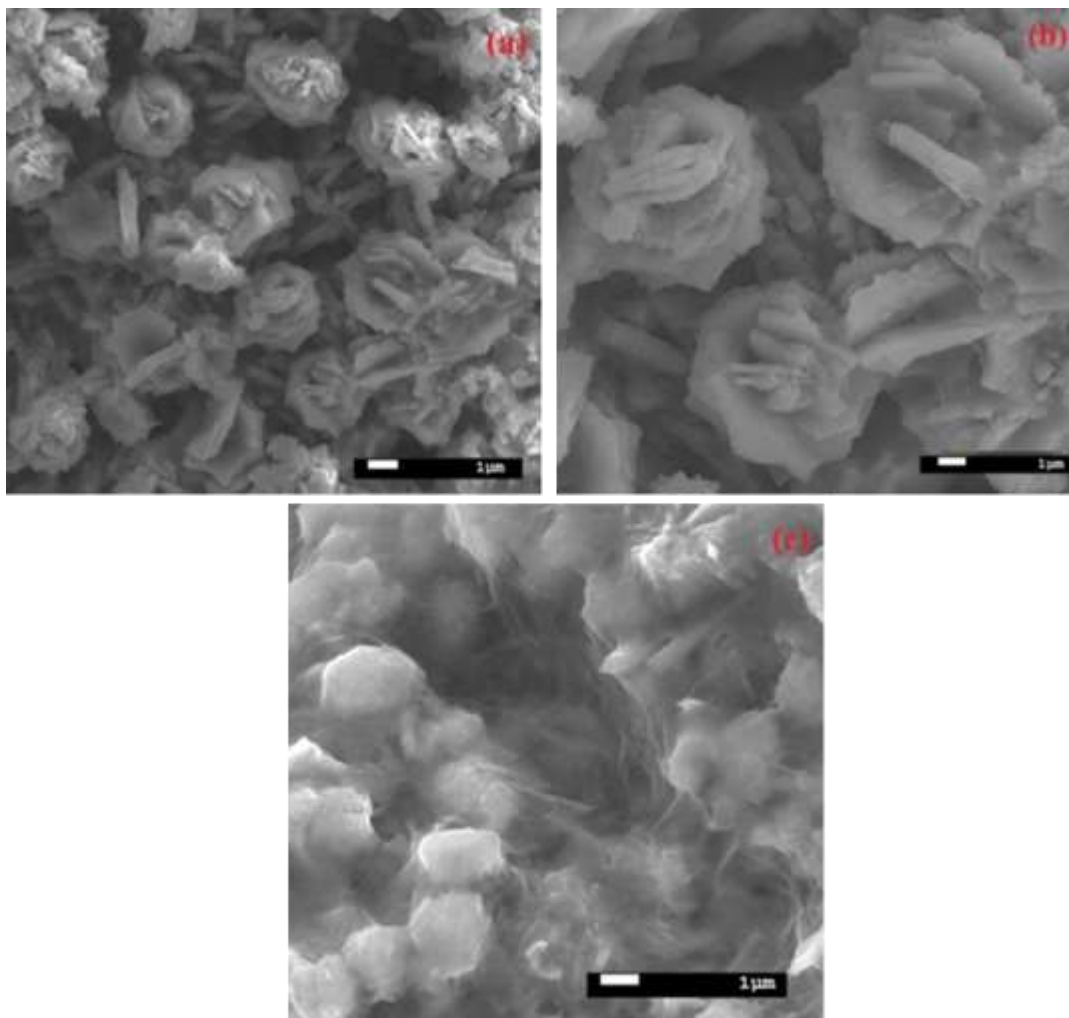

Figure 4. Surface morphology of a)$Zn_{0.075}Cu_{0.025}O$, b)$Zn_{0.050}Cu_{0.050}O$ and c) $Zn_{0.025}Cu_{0.075}O$ nanoparticles

The decreased Cu concentration caused an increase sizes of petal formations from 1 μm to 1.5 μm and nanorod forms decreased, implying deteriorating crystallinity, which caused the petal sizes to increase. Similar results were reported by Drummer et. al for transition metal oxide nanoparticles (Drummer et al., 2021). Particle shape deterioration was observed in $Zn_{0.025}Cu_{0.075}O$ samples with a possible increase in hydroxide formations, since the ratio of copper reached solution and formed residual precipitation, however the x-ray patterns of these samples could not be indexed. Therefore it was difficult to measure the average grain size from the less-resolved SEM images in $Zn_{0.025}Cu_{0.075}O$ nanoparticles.

3.4. Optical Properties

Optical transparency spectra of $Zn_{0.07}Cu_{0.03}O$ and $Zn_{0.04}Cu_{0.06}O$ nanoparticles was shown in Fig.5 between 300-900 nm range. All of the nanoparticles showed sharp absorption edge between 350-380 nm range while

pure ZnO had an absorption edge at 400 nm. In higher (x=0.075) and optimal (x=0.050) Cu concentrations, the optical absorption edge was at 350 nm.
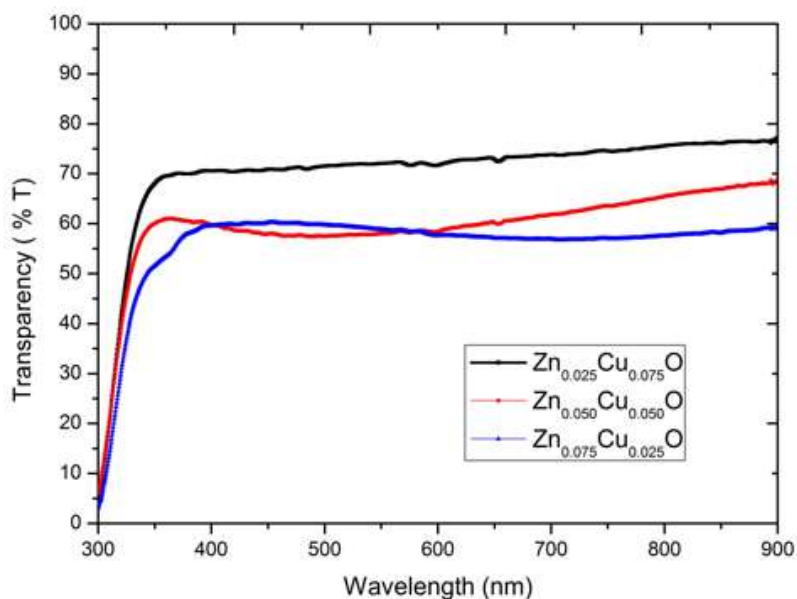

Figure 5. Uv-Vis spectrum of Cu doped ZnO nanoparticles

Optical transparency increased with increase of copper concentration. By decreasing copper concentration to x=0.025, the optical absorption edge shifted slightly to the higher wavelength from 350 nm to 375 nm which was defined as blue shift phenomenon (Gahlahut et al., 2016). The absorption edge shifted towards lower wavelength with the increase of metal dopant so optical absorption edge shifted to lower wavelengths (Liu & Zang, 2018). Some impurity based weak peaks were observed at 570 nm and 650 nm. Optical band gap measurement of the samples was determined by using Tauc plot for direct band gap (n=2) from optical absorption values between 300-900 nm range. An increase of optical band gap was observed by the decreasing Cu concentration that correlated to blue shift. This decrease of band gap was consistent to study of (Ma et.al., 2019). The decrease in the optical band gap of ZnO:Cu with increasing Cu doping indicates that copper settles in the zinc crystal. The fact that the electronegativity of zinc atoms is lower than that of copper atoms can also be shown as a reason for this effect. In another case, it can be said that the concentration of majority carriers and changes in the electronic structure of the material cause this decrease. As the size of nanoparticles decreases, surface and interfacial effects become important and the optical band gap structure changes. This in turn affects the optical band gap of nanoparticles.
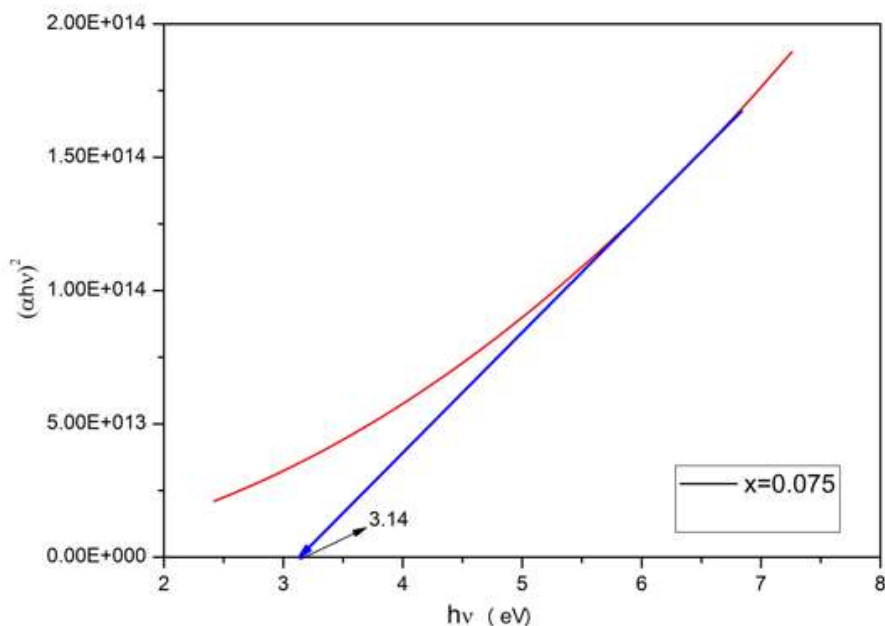
Figure 6. Optical band gap of $Zn_{0.025}Cu_{0.075}O$ nanoparticles

Table 2
Optical band gap of Cu doped ZnO nanoparticles

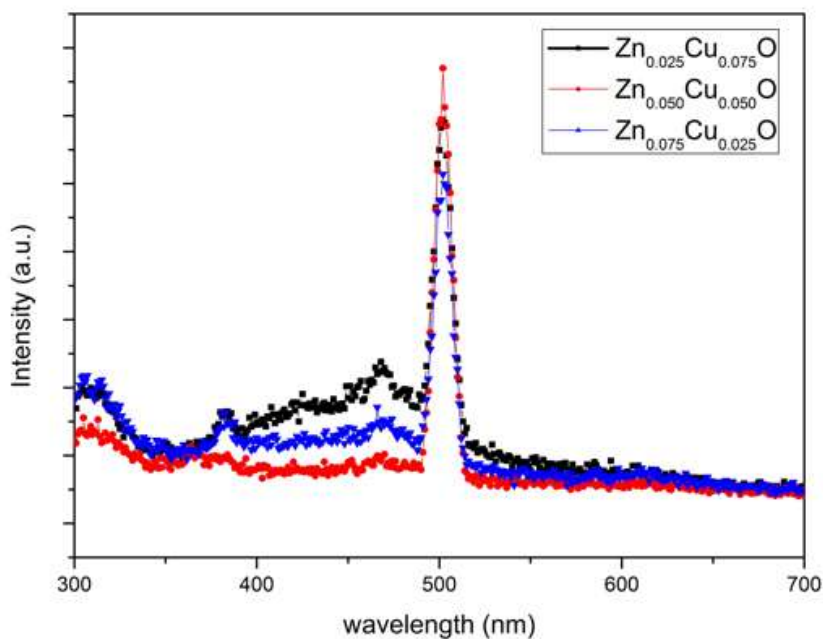| Sample	Optical band gap (eV)
$Zn_{0.075}Cu_{0.025}O$	3.28
$Zn_{0.050}Cu_{0.050}O$	3.23
$Zn_{0.025}Cu_{0.075}O$	3.14

Figure 7. Photoluminescence (PL) spectrum of Cu doped ZnO nanoparticles in the 300-700 nm range

In Fig.7., PL spectrum of Cu doped ZnO nanoparticles were shown in the range between 300-700 nm. All synthesized nanoparticles exhibited three major emission peaks at 389 nm, this UV region peak was attributed to donor–acceptor pair transition (Raji & Gophchandran, 2017). It was interesting that peak intensity was similar for x=0.075 and x= 0.025 and decreased for x=0.050. It may be explained that the peak intensity of PL varied depending on the ratio of dopant materials due to photogenerated electrons occupy shallow trap centers due to the substitution of Zn^{2+} ions by Cu^{2+} ions (Sarf & Kızıl, 2021). Other two peaks were at 485 nm and 502 nm in the visible region and showed the transition between oxygen vacancies and oxygen interstitial defects (Duofa & Zhang, 2009). The slight shift peak was observed a 485 nm with increasing Cu concentration from x= 0.025 to x=0.075 so band gap narrowing was shown in Table 2 (Kamarulzaman et al., 2015). These results were consistent with similar studies in the literature (Kamarulzaman et al., 2015) and (Chang et al., 2010).

4. Conclusion

The present study was conducted to obtain Cu:ZnO nanoparticles by precipitation technique from chemical bath deposition wastes and to characterize the samples by various techniques to determine their size, morphology, band gap and defect energy states. Divalent Cu^{2+} ions were well substituted into Zn^{2+} sites and maintained ZnO crystallinity. Although elemental analysis confirmed that the presence of Cu (w%), X-ray patterns of Cu:ZnO samples showed any other Cu related phase as a result, doping process was successful. Doping of Cu to ZnO had a strong effect on the size and morphology of the samples, as a result, the optical and PL properties also varied accordingly.

Conflicts of Interest

The author declares no conflict of interest.

References

Anitha, S., & Muthukumaran, S. (2020). Structural, optical and antibacterial investigation of La, Cu dual doped ZnO nanoparticles prepared by co-precipitation method. *Materials Science and Engineering: C*, *108*, 110387. doi:10.1016/j.msec.2019.110387

Bordbar, M. , Khodadadi1, B., Mollatayefe, N., Yeganeh A., (2017). Influence of metal (Ag, Cd, Cu)-doping on the optical properties of ZnO nanopowder: Variation of band gap *Journal of Applied Chemistry, 8* (2013) 43-47

Chu, V. B., Siopa, D., Debot, A., Adeleye, D., Sood, M., Lomuscio, A., … Dale, P. J. (2021). Waste- and Cd-Free Inkjet-Printed Zn(O,S) Buffer for Cu(In,Ga)(S,Se)2 Thin-Film Solar Cells. *ACS Applied Materials & Interfaces*, *13*(11), 13009–13021. doi:10.1021/acsami.0c16860

Das, B. K., Das, T., Parashar, K., Thirumurugan, A., & Parashar, S. K. S. (2017). Structural, bandgap tuning and electrical properties of Cu doped ZnO nanoparticles synthesized by mechanical alloying. *Journal of Materials Science: Materials in Electronics*, *28*, 15127-15134.

Debanath, M. K., & Karmakar, S. (2013). Study of blueshift of optical band gap in zinc oxide (ZnO) nanoparticles prepared by low-temperature wet chemical method. *Materials Letters*, *111*, 116–119. doi:10.1016/j.matlet.2013.08.069

Drummer, S., Madzimbamuto T., and Chowdhury M. (2021). Green Synthesis of Transition-Metal Nanoparticles and Their Oxides: A Review *Materials 14*, no. 11: 2700. https://doi.org/10.3390/ma14112700

Gahlaut, U.P.S., Kumar V., Pandey R.K., & Goswami Y.C. (2016) Highly luminescent ultra-small Cu doped ZnO nanostructures grown by ultrasonicated sol-gel route, *Optik 127* 4292–4295.

Istrate, AI., Mihalache, I., Romanitan, C. *et al.* (2021). Copper doping effect on the properties in ZnO films deposited by sol–gel. *J Mater Sci: Mater Electron* 32, 4021–4033 (2021). https://doi.org/10.1007/s10854-020-05144-2

Kamarulzaman, N., Kasim, M.F. & Rusdi, R. (2015). Band Gap Narrowing and Widening of ZnO Nanostructures and Doped Materials. *Nanoscale Res Lett* 10, 346. https://doi.org/10.1186/s11671-015-1034-9

Kim, C. E., Moon, P., Kim, S., Myoung, J.-M., Jang, H. W., Bang, J., & Yun, I. (2010). Effect of carrier concentration on optical bandgap shift in ZnO:Ga thin films. *Thin Solid Films*, *518*(22), 6304–6307. doi:10.1016/j.tsf.2010.03.042

Labhane, P. , Huse, V. , Patle, L. , Chaudhari, A. and Sonawane, G. (2015) Synthesis of Cu Doped ZnO Nanoparticles: Crystallographic, Optical, FTIR, Morphological and Photocatalytic Study. *Journal of Materials Science and Chemical Engineering*, 3, 39-51. doi: 10.4236/msce.2015.37005.

Liu, W. L., & Zhang, Y. F. (2018). Blueshift of absorption edge and photoluminescence in Al doped ZnO thin films. *Integrated Ferroelectrics*, *188*(1), 112–120. doi:10.1080/10584587.2018.1454222

Ma, Z., Ren, F., Ming, X., Long, Y., & Volinsky, A. A. (2019). Cu-Doped ZnO Electronic Structure and Optical Properties Studied by First-Principles Calculations and Experiments. Materials, 12(1). doi:10.3390/ma12010196

Malinowska, B., Rakib, M. & Durand, G. (2002). Cadmium recovery and recycling from chemical bath deposition of CdS thin layers. *Prog. Photovolt. Res. Appl. 10*, 215–228. https://doi.org/10.1002/pip.402.

Naik, E. I., Naik, H. S. B., Swamy, B. E. K., Viswanath, R., Gowda, I. K. S., Prabhakara, M. C., & Chetankumar, K. (2021). Influence of Cu doping on ZnO nanoparticles for improved structural, optical, electrochemical properties and their applications in efficient detection of latent fingerprints. *Chemical Data Collections*, *33*, 100671. doi:10.1016/j.cdc.2021.100671

Raji, R., & Gopchandran, K. G. (2017). ZnO:Cu nanorods with visible luminescence: copper induced defect levels and its luminescence dynamics. *Materials Research Express*, *4*(2), 025002. doi:10.1088/20531591/aa5762

Sarf, F., Karaduman E.I., Yakar, E., & Acar, S., (2021). Substrate critical effect on the structural and H2 Gas sensing characteristics of solution-processed Zn0.075Cu0.025O films, *Mater. Res. Express, 8,* 126401, DOI: 10.1088/2053-1591/ac3f09.

Sarf, F., & Kızıl, H., (2021). Defect Emission Energy and Particle Size Effects in Fe:ZnO Nanospheres Used in Li-ion Batteries as Anode. *Journal of Electronic Materials* , vol.10, 111.

Vasudevan, J;, Johnson, S; Jeyakumar, B; et al, *Materials Today: Proceedings,* 2021, 12-19

Vasudevan, J., Johnson Jeyakumar, S., Arunkumar, B., Jothibas, M., Muthuvel, A., & Vijayalakshmi, S. (2022). Optical and magnetic investigation of Cu doped ZnO nanoparticles synthesized by solid state method. *Materials Today: Proceedings, 48*, 438–442. doi:10.1016/j.matpr.2020.12.429

Wang, L.(2019). *European Patent Application Bulletin 26*, 26.06.2019

Wang, D.F., Zhang, T.,(2009). Study on the defects of ZnO nanowire, *Solid State Communications*, *149*:1947-1949